ASME Journal of Engineering for Gas Turbines and Power
Online journal at:
https://asmedigitalcollection.asme.org/gasturbinespower

Techno-Economic Comparative Assessment of High-Temperature Heat Pump Architectures for Industrial Pumped Thermal Energy Storage

Silvia Trevisan[1]
Department of Energy Technology,
KTH Royal Institute of Technology,
Brinnellvägen 63,
Stockholm 100 44, Sweden
e-mail: trevisan@kth.se

Bjarke Buchbjerg
KYOTO Group AS,
Fornebuveien 1,
Lysaker 1366, Norway
e-mail: bjarke@kyotogroup.no

Arne Höeg
ENERIN AS,
Torvveien 1,
Asker 1383, Norway
e-mail: arne@enerin.no

Rafael Guedez
Department of Energy Technology,
KTH Royal Institute of Technology,
Brinnellvägen 63,
Stockholm 100 44, Sweden
e-mail: rafael.guedez@energy.kth.se

The industrial sector is a key global source of wealth, but it is also recognized as a major challenge toward worldwide decarbonization. Today, the industrial sector requires more than 22% of the global energy demand as thermal energy and produces for this about 40% of the total CO_2 emissions. Solutions to efficiently decarbonize the industrial sector are deemed. This work presents a comparative techno-economic performance assessment of a high-temperature heat pump (HTHP) integration within a molten salts (MSs) based power-to-heat system for industrial heat flexible generation. The main system performance is reported in terms of required working conditions and temperature for the heat pump and thermal demand size as well as reduction of the attainable levelized cost of heat (LCoH) against nonflexible electric boiler based systems. The impact of different industrial load profiles, electricity prices, heat pump capital cost, and heat pump real to Carnot efficiency ratio are also presented. The results highlight that the proposed system can be cost-competitive, particularly for thermal demand around 10 MW and waste heat temperatures above 80 °C. Under these conditions, LCoH reductions higher than 15%, with respect to the considered nonflexible electric boiler alternative, are attainable. These LCoH reductions are primarily driven by savings in electrical consumption as high as 30%. This study sets the ground for further power-to-heat techno-economic investigations addressing different industrial sectors and identifies main system and components design strategies, integrations, and targets. [DOI: 10.1115/1.4066989]

Introduction

The industrial sector is one of the main global greenhouse gases emitters [1], and it is considered a key challenge toward attaining a decarbonized society in the near future [2]. Today, about 50% of global energy consumption is spent for heating purposes, and about 44% of this is required by the industrial sector [3]. For the low and medium temperature industrial thermal load, a typical demand is saturated or superheated steam in the temperature range between 150 °C and 400 °C. More than 80% of this demand is currently covered by fossil fuel sources. Efficient and cost-effective solutions addressing the industrial thermal demand are needed and potentially available. However, required elevated initial investments often represent major hurdles to be faced for a relevant market uptake.

Electrification is a key pathway to attain a decarbonized society, by cost-effectively contributing to fossil fuel substitution and renewable integration [4]. The technological potential for industry electrification has been estimated in Ref. [5] showing that 78% of the heating demand could be fulfilled by commercial technology. Electrification could also reduce the industry's greenhouse gas emissions by more than 75% [6]. Power-to-heat systems including thermal energy storage (TES) can maximize the exploitation and consumption of fluctuating renewable power while ensuring reliable heat generation for the industry. The development of very high-temperature heat pumps (HTHPs) delivering a sink side temperature higher than 150 °C is currently a major R&D topic with several lab scale and pilot solutions being developed and verified [7]. In comparison with direct electric heating (electric boilers), HTHP can provide higher efficiency (called coefficient of performance (COP) in the HTHP context) [8]. The exploitation of TES based systems including HTHP can represent a major step forward toward the industrial mid temperature heat decarbonization [9]. Such system can largely reduce the industry dependency on fossil fuels, minimize its operational costs, while providing a source of flexibility to the overall grid and facilitating the integration of fluctuating renewable energy sources. However, comprehensive techno-economic assessments of power-to-heat systems including TES and HTHP are rare, particularly when focusing on the industrial sector [10]. Therefore, targets for the units and components development are also missing.

This work, also starting from the results of previous authors' research [11], aims at filling this research gap and presents the techno-economic comparative assessment of a flexible HTHP and

Turbo Expo, June 24–28, 2024. GT2024.
[1]Correponding author.
Manuscript received August 23, 2024; final manuscript received September 11, 2024; published online December 20, 2024. Editor: Jerzy T. Sawicki.

molten salts (MSs) TES based power-to-heat system. The proposed system stores thermal energy at about 400 °C and provides saturated steam at 180 °C. Typical major industrial users of steam, such as paper and cardboard industries, are considered together with their typical consumption patterns.

The system's performance is assessed comparatively, against commercial alternatives such as nonflexible electric and natural gas (NG)-based boilers on the basis of technical and economic indicators. A set of sensitivity analyses is also performed to highlight the relevance and impact of key assumptions: thermal load and its daily pattern, electricity prices and its fluctuation, HTHP capital costs (CAPEX), and HTHP real to Carnot efficiency ratio.

Materials and Methods

This section describes the main methods and modeling activities followed in this work. All main assumptions are also summarized.

Integrated System Definition. The investigated system is sketched in Fig. 1; the main parameters describing the system are summarized in Table 1. The investigated system is aimed at upgrading waste heat and low-grade heat via a HTHP, storing high-temperature heat, via a dedicated thermal energy storage unit, and delivering process heat in the form of saturated steam on demand to industrial users. The investigated system includes a Stirling cycle based HTHP which permits to upgrade waste heat stream from a source side in the range 20–120 °C to a sink side up to 400 °C, an inline electric heater (EH), a molten salt (ternary salt with a mass ratio of 43% potassium-nitrate (KNO_3), 15% sodium-nitrate ($NaNO_3$), and 42% calcium nitrate ($Ca(NO_3)_2$), [12]) based modular TES, and a MS based steam generator. The modular TES, steam generator, and inline electric heater have been described in details in previous works [11,13] by the authors, and the same modeling methodology has been used in this work. The HTHP deploys a Stirling cycle with He as the internal working fluid, ensuring elevated performance and zero global warming potential associated with the working fluid. A Stirling based unit has been selected as potentially more scalable and suited for small to medium industrial clients than alternative turbomachinery-based units. Additional details on the considered HTHP units have been presented in Ref. [14]. The HTHP and EH are installed in series. The EH boosts the molten salts temperature up to the required maximum temperature of 400 °C after leaving the hot side of the heat pump, in case the HTHP cannot reach these elevated sink side temperatures.

Thermodynamic Modeling. The system thermodynamic performance has been modeled and assessed in a static approach considering energy balancing and neglecting transient behaviors. Specifically, the net COP of the HTHP has been defined as in the following equation:

$$\mathrm{COP}_{\mathrm{Net}} = \frac{T_h}{T_h - T_c} \cdot \eta = \frac{Q_{\mathrm{sink}}}{P_{\mathrm{el}}} \tag{1}$$

Table 1 Main system parameters

Parameter	Value	Unit
HTHP source temperature, T_c	20–120	°C
HTHP sink temperature, T_{sink}	200–400	°C
MS minimum temperature	170	°C
MS maximum temperature	400	°C
Electric heater efficiency	98	%

where T_h and T_c are the sink and source side temperatures for the HTHP (with T_h in the range 200–400 °C and T_c in the range 20–120 °C), η is the net to Carnot COP ratio, assumed equal to 0.6 (as from preliminary experimental results shown in Ref. [14]), Q_{sink} is the thermal power delivered to the sink (hot) side, and P_{el} is the electric power required. The specific $\mathrm{COP}_{\mathrm{Net}}$ map is shown in Fig. 2.

The investigated system heats the molten salts and, in doing so, charges the TES, via operating in series the HTHP and the EH. The EH boosts the molten salts temperature up to the required 400 °C after leaving the hot side of the heat pump. Such arrangement can enable higher electricity savings and general tradeoff between expensive HTHP and cheaper but less efficient EH units. The EH is deployed in the high-temperature range since the HTHP costs and performance are negatively affected by operating it at higher working temperatures. During charge, the share of thermal power, σ, provided by the HTHP and the EH depends on T_{sink}, the maximum temperature achieved by the HTHP in its sink side, and is defined as in the following equations:

$$\sigma_{\mathrm{HTHP}} = \frac{T_{\mathrm{sink}} - T_{\mathrm{min}}}{T_{\mathrm{max}} - T_{\mathrm{min}}} \tag{2}$$

$$\sigma_{\mathrm{EH}} = 1 - \sigma_{\mathrm{HTHP}} \tag{3}$$

The share of electric power consumed by the HTHP and the EH is instead dependent on both the source and sink temperatures of the HTHP as directly related to the COP of the HTHP. Figure 3 summarizes the percentual electric power consumed by the HTHP at different operating conditions, and it also visualizes the difference between the share of thermal power (σ_{HTHP}). Wider differences between the thermal and electric power share are visible in the range of operating conditions ensuring higher COP for the HTHP.

The system's performance has been investigated considering three typical industrial thermal demand profiles: "profile A" representative of a single shift with constant load between 08.00 and 18.00 only during working days (5 days/week); "profile B" representative of a double shift with constant load between 06.00 and 21.00 everyday; and "profile C" representative of a continuous demand with constant load 24 h/day every day. The profiles are summarized, in their nondimensional fashion, in Fig. 4. The three profiles are characterized by three daily operative hours: $h_{\mathrm{op,A}}$ equal to 10, $h_{\mathrm{op,B}}$ equal to 16, and $h_{\mathrm{op,C}}$ equal to 24. Additionally, different thermal load demands have been considered as representative of

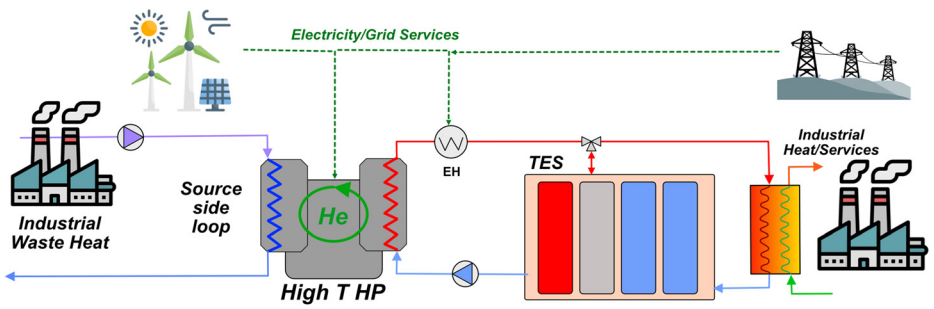

Fig. 1 Integrated system layout sketch

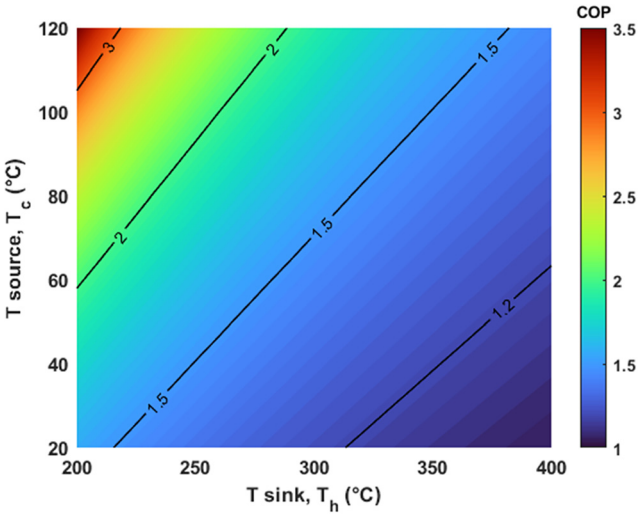

Fig. 2 Considered HTHP net COP map for different source and sink side working temperatures

typical small to medium industries which could benefit from the proposed system. Specifically, the base industrial thermal demand, Q_{load}, has been considered equal to 0.2, 0.5, 1, 3, 5, 10, 15, and 20 MW_{th} and applied as from the above profiles.

To emulate specific system charging patterns during typical periods at low electricity prices, a base charging time, h_{ch}, of 8 h has been considered. Depending on the specific industrial demand profile, the charging occurs primarily during the night or partially simultaneously during discharge. To ensure a full reliability of the industrial steam generation, the need for installed thermal charging power between both the HTHP and EH, $Q_{HTHP+EH}$, has been calculated as in the following equation:

$$Q_{HTHP+EH} = Q_{load} \frac{h_{op,x}}{h_{ch}} \tag{4}$$

where Q_{load} is the nominal thermal power demand on the industrial site, $h_{op,x}$ is the operational hours of the specific profile simulated (A, B, or C), and h_{ch} is the available charging time at low electricity prices.

The total installed thermal charging power $Q_{HTHP+EH}$ is then allocated to the HTHP or the EH depending on the specific working

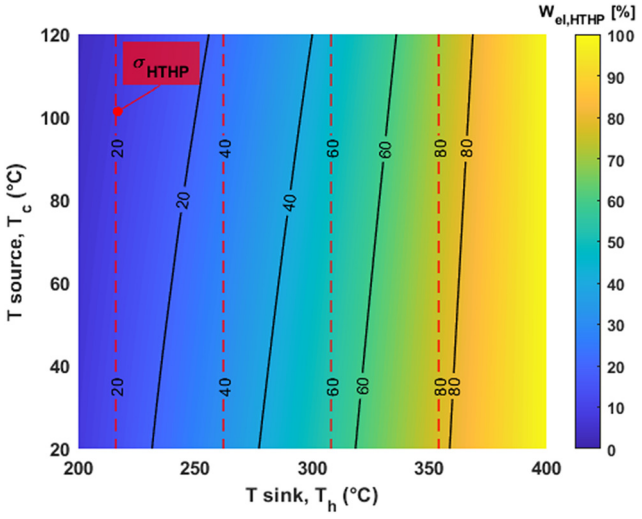

Fig. 3 Percentual share of electric power consumed by the HTHP at different sink and source temperature. Also highlighted the HTHP thermal power share σ_{HTHP} (dashed lines).

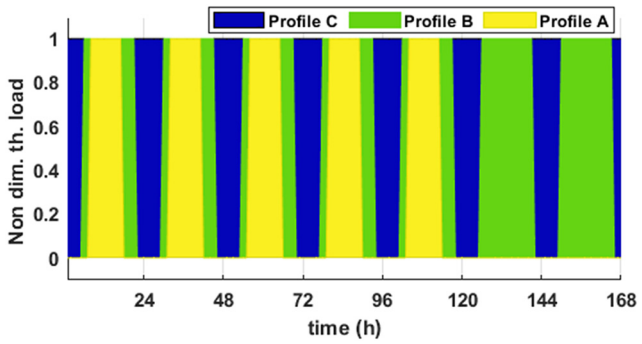

Fig. 4 Nondimensional thermal load profiles considered (shown as over posed)

conditions as described by the shares σ_{HTHP} and σ_{EH}, as from the following equations:

$$Q_{HTHP} = \sigma_{HTHP} \cdot Q_{HTHP+EH} \tag{5}$$

$$Q_{EH} = \sigma_{EH} \cdot Q_{HTHP+EH} \tag{6}$$

To ensure proper charging of the system during the limited cheap electricity hours during the day, the installed thermal charging power must be increased with respect to the actual thermal load.

The system's performance has been benchmarked and compared against the once attainable by alternative solutions including: a main business as usual (BAU) case employing a electric boiler without flexibility asset, a system similar to the described one, including the MS TES, but without the HTHP, only using a main EH to charge the unit, and a NG-based boiler without flexibility asset. The alternative system including TES charges the unit during h_{ch}, while the alternative solutions without flexibility assets operate during the full operative hours of the studied industrial demand profile. Table 2 summarizes the main technical and economic parameters considered for the alternative cases and for the benchmarking.

Economic System Modeling. The economic aspects have been described following the approach described by the authors in Ref. [11]. The capital expenditure, CAPEX, has been calculated in a bottom-up approach summing up the capital costs of all main equipment. Specifically, the HTHP CAPEX has been calculated defined from the data shown in Ref. [15] and scaled to account for different operating temperatures and thermal load, as from the following equation:

$$C_{HTHP} = c_{ref,HTHP} \cdot Q_{sink} \left(\frac{T_{sink} + 273.15}{T_{ref} + 273.15} \right)^{\alpha} \tag{7}$$

where $c_{ref,HTHP}$ is the reference specific HTHP CAPEX gathered from Ref. [15], T_{ref} has been considered equal to 150 °C, and α has been considered equal to 0.5. The resulting HTHP specific CAPEX (C_{HTHP}/Q_{sink}) is shown in Fig. 5.

The specific EH cost has been considered equal to 50 €/kW_e, while the cost model for the TES unit has been considered equal to the one shown in Ref. [11]. The main parameters describing the comparative cases are summarized in Table 2. In particular, a specific electric boiler cost of 73 €/kW has been considered [16]. Instead, null capital cost has been considered for the NG boiler assuming that this represents the widespread solution within the industrial environment. Thus, from the industrial user's perspective, such an alternative is primarily characterized by its operational costs.

The operational costs, OPEX, account primarily for the electricity costs due to system charging, for which an electricity average base cost of 75 €/MWh has been assumed. This price is assumed during the cheap charging hours, h_{ch}. Instead, for the nonflexible

Table 2 Main technical and economic parameters for comparative alternatives

Parameter	Value	Unit
Electric boiler efficiency	95	%
NG boiler efficiency	85	%
Electric boiler specific CAPEX	73	€/kW$_e$
Electric boiler auxiliary OPEX	2	%
NG boiler auxiliary OPEX	5	%
Electricity price penalty, β	30	%
NG price	82.6	€/MWh
CO_2 tax (average EU emission trading system (ETS) market price)	88.46	€/ton$_{CO_2}$
Electric grid equivalent CO_2	100	g$_{CO_2}$/kWh

alternatives (electric and NG boiler), a penalty, equal to 30%, on the electricity price during the extra hours needed beside h_{ch} has been included. The auxiliary consumptions related costs, equal to 2–5% of the charging related electricity costs, have also been included. No cost has been considered associated with the heat required at the source side of the HTHP, as it would come from waste heat sources. For the NG boiler, an additional OPEX source due to the direct CO_2 emissions has been included. The specific cost for the emitted CO_2 has been considered equivalent to the average CO_2 allowance in the EU Emission Trading System in 2023 [17]. Thus, the OPEX for the investigated system has been expressed as in Eq. (8), while the OPEX for the alternative electric boiler and NG boiler have been calculated as in Eqs. (9) and (10)

$$\mathrm{OPEX} = (1 + \mathrm{aux}) \cdot (h_{ch} \cdot d_{op,x} \cdot 52) \cdot p_{el} \cdot W_{el,TOT} \tag{8}$$

$$\mathrm{OPEX}_{\mathrm{El\ Boiler}} = (1 + \mathrm{aux}) \cdot 52 d_{op,x} \cdot p_{el} \cdot W_{\mathrm{El\ Boiler}} \left[h_{ch} + (h_{op,x} - h_{ch})(1 + \Delta p_{el})\right] \tag{9}$$

$$\mathrm{OPEX}_{NG} = (1 + \mathrm{aux}_{NG}) \cdot (h_{op,x} \cdot d_{op,x} \cdot 52) \cdot p_{NG} \cdot Q_{NG} + t_{CO_2} \cdot \mathrm{CO_{2NG}} \tag{10}$$

where aux is the auxiliary consumptions related costs, $d_{op,x}$ are the weekly operating days (equivalent to 5 for profile A and 7 for profiles B and C), W is the electric power consumption from the HTHP and EH or from the electric boiler, Δp_{el} is the introduce penalty equivalent to an increase of 30% of the electricity price for the nonflexible alternatives, p_{NG} is the cost of NG, Q_{NG} is the thermal power required in the NG boiler, tCO_2 is the carbon tax, and CO_{2NG} is the emitted equivalent CO_2 from the NG boiler [18–24].

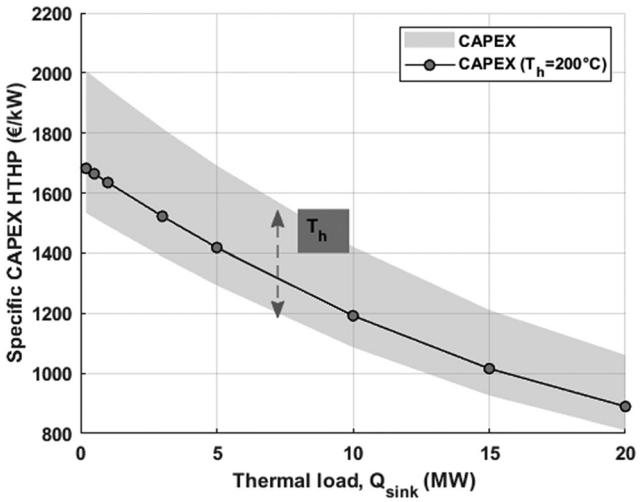

Fig. 5 Specific CAPEX range of the HTHP as a function of the sink thermal load and sink temperature

The levelized cost of heat (LCoH) attained by the investigated system has been considered as the main techno-economic performance indicator. The LCoH of the investigated system has been calculated as in the following equation:

$$\mathrm{LCoH} = \frac{\mathrm{CAPEX} + \sum_{n=1}^{N_{op}} \frac{\mathrm{OPEX}}{(1+d)^n}}{\sum_{n=1}^{N_{op}} \frac{E_{load}}{(1+d)^n}} \tag{11}$$

where N_{op} is the full lifetime of the plant equal to 25 yr, d is the considered discount rate of 5%, and E_{load} is the yearly thermal energy delivered to the industrial site.

The benchmarking against the alternative solutions, represented primarily by the electric boiler, has been carried out considering both the electric consumption and the attainable LCoH. The two main indicators, ΔW_{el} and ΔLCoH, are summarized by Eqs. (12) and (13). Similarly, the savings in CO_2 emissions have been considered, as defined in Eq. (14)

$$\Delta W_{el} = \frac{W_{el} - W_{el,BAU}}{W_{el,BAU}} \tag{12}$$

$$\Delta\mathrm{LCoH} = \frac{\mathrm{LCoH} - \mathrm{LCoH_{BAU}}}{\mathrm{LCoH_{BAU}}} \tag{13}$$

$$\Delta\mathrm{CO_2} = \frac{\mathrm{CO_2} - \mathrm{CO_{2,BAU}}}{\mathrm{CO_{2,BAU}}} \tag{14}$$

Finally, a set of sensitivity analyses has been performed to assess the relevance and impact of some key assumptions and enlarge the applicability of the results to a larger set of potential user cases. As previously mentioned, different specific thermal load and different industrial thermal load profiles have been studied. The impact of different electricity prices and available cheap charging hours, as well as the specific CAPEX of the HTHP and the real to Carnot efficiency ratio of the HTHP, have been considered. Specifically, electricity prices equal to 50 €/MWh, 75 €/MWh (equivalent to the base case), and 100 €/MWh have been considered. Available charging hours between 6 and 10 h/day have been simulated. HTHP CAPEX equivalent to 75% and 125% of the costs shown in Fig. 5 have been considered. Real to Carnot efficiency ratio of 0.5, 0.6 (equivalent to the base case), and 0.7 have also been modeled. In each set of sensitivity analyses, all other parameters have been kept constant and equivalent to the base case.

Results and Discussion

This section presents and discusses the main results. First, the main techno-economic results for a base case are shown in a comparative manner against electric boiler based BAU. Second, the outcomes of a set of sensitivity analyses are presented and discussed.

Base Case. Figure 6 summarizes the attainable electric consumption savings ΔW_{el} with respect to an electric boiler considering different waste heat source temperatures as well as different maximum sink temperatures attained by the HTHP. For sake of completeness, Fig. 6 also reports, as solid contours, the electric consumption saving attainable by a flexible system integrating TES and EH, but without the HTHP. Within the considered operative range, the maximum electric consumption savings, higher than 30%, are attained at the highest source temperature and HTHP sink temperature. Under these temperature conditions, the HTHP contribution and share σ_{HTHP} is maximized, as shown in Fig. 3, and the HTHP COP is around 1.4, higher than for lower T_{source}. A reduction in either the source or the sink temperature leads to reductions of the electric consumptions savings, down to about 10%. Specifically, a reduction of the source side temperature negatively

impacts the COP of the HTHP, as shown in Fig. 2. A decrease of the Tsink causes lower contributions of the HTHP to the system charging, σ_{HTHP}, which can go down to below 20%, as shown in Fig. 3, and which are not compensated by the increase of the HTHP COP.

Thus, the proposed solution can attain relevant electricity consumption savings. However, it should be highlighted that the additional HTHP accounts for about 40–80% of the total CAPEX of the system depending on the specific operating temperatures and sizing. Particularly, higher sink temperature would lead to more expensive HTHP as shown by Eq. (7). The HTHP is a major CAPEX source, reducing the cost relevance of the MS based TES unit. This suggests that the presented results would also be suitable and adaptable to other TES technologies.

Figure 7 shows the benchmarking of the proposed system in terms of LCoH for a unit covering 5 MW of thermal load following profile B. The range of LCoH for the proposed system depends on the specific working conditions of the HTHP (source and sink temperatures, as further elaborate later). A similar system without HTHP and only including an EH for the charging (EH + TES), an electric boiler, and an NG boiler are considered. The electric boiler is considered as the primary comparative unit since it provides intermediate performance, and it can be considered as a relevant business as usual or preferred path toward electrification. Depending on the specific operating conditions, the proposed system can attain lower LCoH than all comparative cases. The investigated systems can lead to LCoH as low as 70.4 €/MWh. It is important to highlight that both EH + TES and electric boiler can attain LCoH within the range of the ones recorded by the proposed system. Therefore, each potential installation should be properly evaluated, and the specific working conditions for the HTHP should be carefully considered to ensure that its investment is adequately compensated by the improved performance. NG boiler is instead largely outcompeted by the proposed system, as well as by the other investigated solutions.

Figure 8 summarizes the range of attainable CO_2 savings by the proposed system with respect to the aforementioned alternatives: a similar system without the HTHP and only relying on the EH for the charge (EH + TES), a nonflexible electric boiler, and a NG boiler. For electricity-based systems (EH + TES and electric boiler), the CO_2 emission savings are directly linked to the savings in electricity consumption and ranges between 5% and 50% depending on the specific working conditions of the HTHP. The proposed system could instead lead to CO_2 savings between 50% and 72% with respect to NG boiler, thus largely contributing to the industrial decarbonization. Even higher savings with respect to the NG boiler

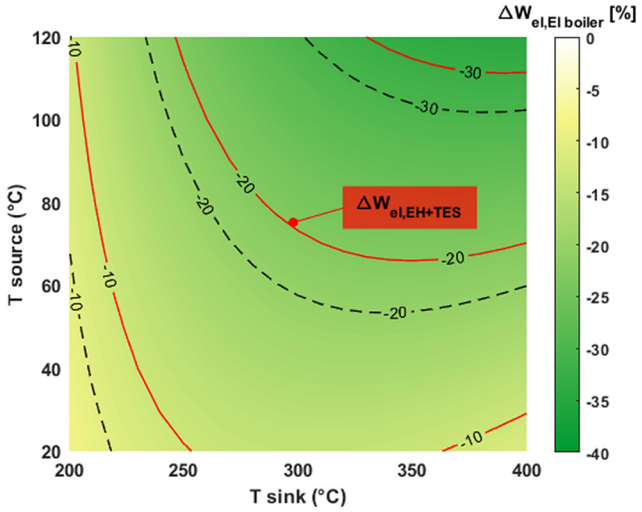

Fig. 6 Electric consumption savings attained by the investigated system against an electric boiler unit (dashed contour and main color) and TES + EH (flexible power-to-heat without HTHP—solid contour)

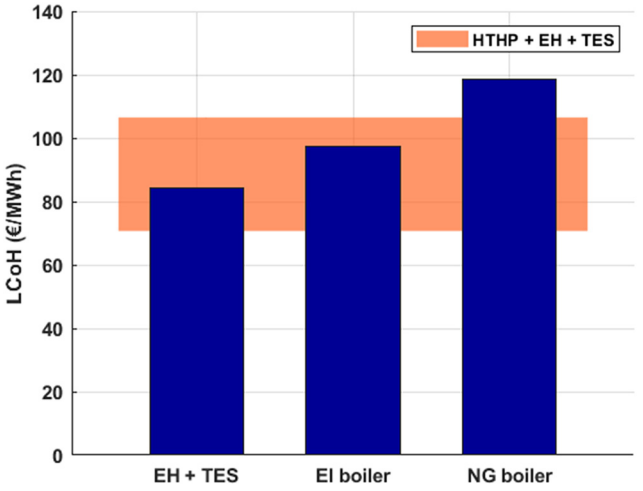

Fig. 7 LCoH benchmarking for the proposed system against alternative solutions

alternative could be attained in a future with greener electricity production and lower foreseen electricity grid CO_2 equivalent factors.

Figure 9 provides more insights on the relevance and attainable techno-economic performance of the proposed system under different industrial thermal profiles and specific loads. Specifically, Fig. 9 summarizes the attainable LCoH reduction with respect to a comparative electric boiler and the required sink and source side temperatures for the HTHP to attain the minimal LCoH for the proposed system. For limited thermal demand such as simulated by profile A, the proposed system, under the considered working conditions and costs, attains LCoH within a −2% range with respect to electric boilers. Thus, in conditions similar to profile A and particularly at low nominal loads, the elevated investment and complexity of the proposed system are not paid off by the increased system efficiency. For *profile B* and *profile C* even at small scale (i.e., $Q_{load} = 200$–500 kW), LCoH reductions higher than 10% with respect to nonflexible electric boilers are attainable. For industries characterized by continuous thermal demand and elevated load (i.e., $Q_{load} = 20$ MW), LCoH savings of more than 20% are achievable. To attain elevated LCoH savings, particularly at thermal load higher than 10 MW, an increase of the HTHP contribution, σ_{HTHP}, is required. To achieve this, T_{sink} of about 310 °C are needed by both profile B and profile C. In the case of profile C, maximum T_{sink} of 310 °C is required for thermal load of 10 MW, for higher thermal

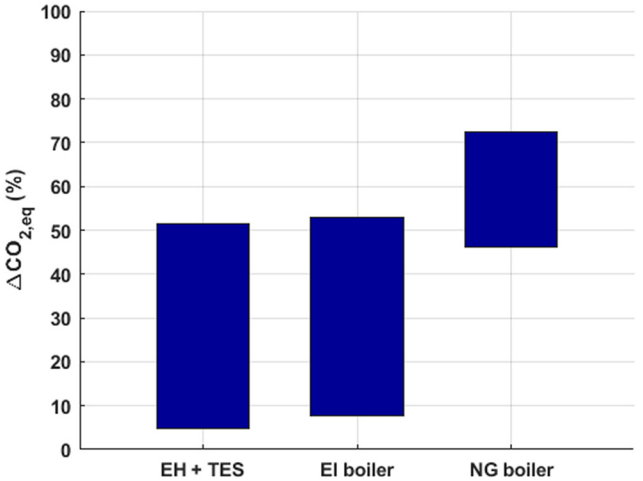

Fig. 8 CO_2 savings attainable by the proposed system with respect to the considered alternatives

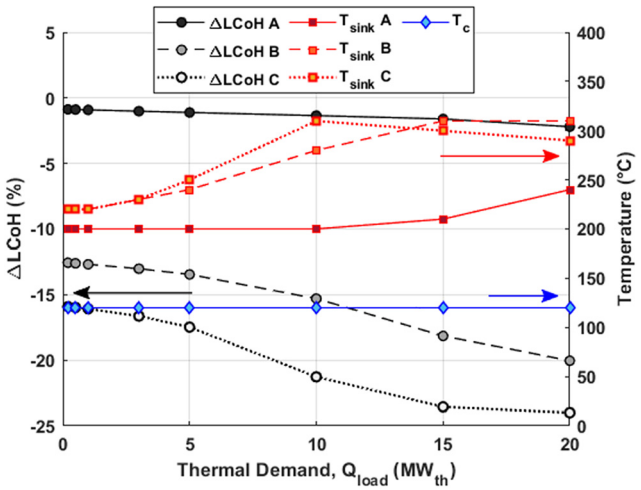

Fig. 9 Maximum attainable LCoH savings and required source and sink temperatures for the HTHP for the three different industrial profiles

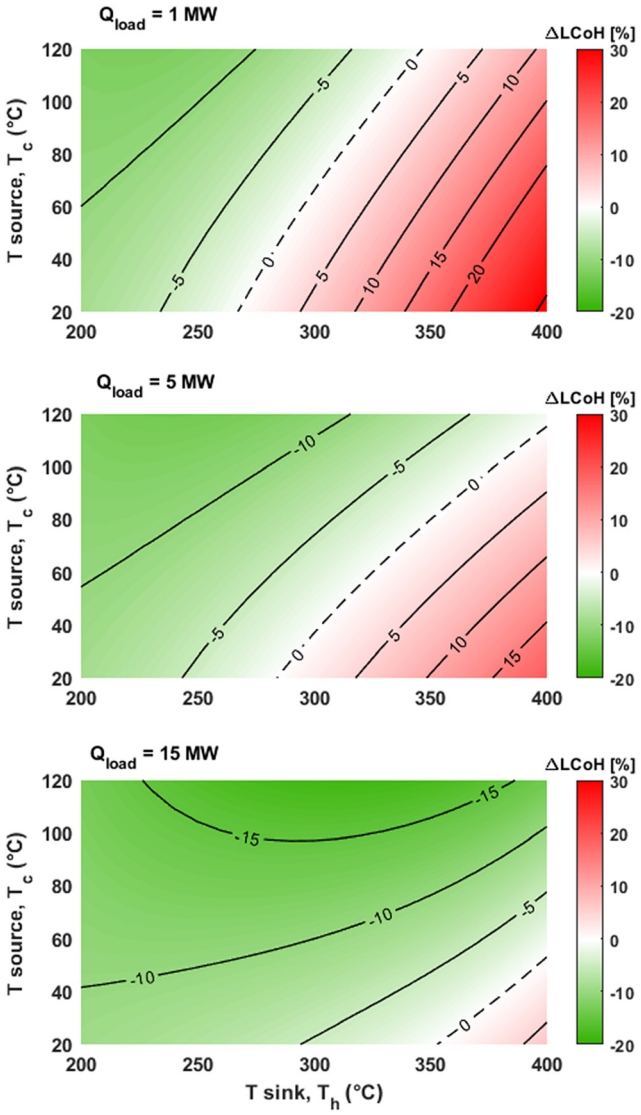

Fig. 10 Attainable LCoH savings for the proposed system for profile B and a Q_{load} equal to 1 MW, 5 MW, and 15 MW with respect to nonflexible electric boilers

load instead a limited reduction of T_{sink} is noted. This reduction is caused by the increase of the HTHP CAPEX at higher T_{sink}, which is not compensated by its improved performance. Regardless of the specific thermal load and profile, the maximum waste heat temperature and source side temperature are preferred to ensure lower temperature lifts for the HTHP and improved performance.

Figure 10 shows the attainable LCoH difference with respect to a nonflexible electric boiler for three based industrial thermal load for profile B. This specific industrial thermal load is highlighted and further considered for most of the performance comparison since it represents a large variety of typical scenarios and it attains intermediate performance between the considered alternative profiles. Due to the elevated CAPEX of the HTHP, the minimal LCoH and maximum LCoH savings are attained based on a tradeoff between HTHP additional costs and HTHP improved performance and consequent electricity savings, which reflect in an OPEX reduction. The proposed system is more cost-competitive the higher the waste heat source side temperature. At small scale (i.e., $Q_{load} = 1$ MW), the investigated system is cost-competitive only at σ_{HTHP} below 40% and T_{sink} lower than 300 °C, which enable relevant electricity consumption savings while limiting the needed investment in the HTHP. At this small thermal load, the exploitation of HTHP for MS preheating could be a valuable and preferable solutions (instead of using the HTHP to cover the full temperature range), providing LCoH reduction of about 10%. For larger scales (i.e., $Q_{load} = 15$ MW), the proposed system becomes more cost-competitive with potential LCoH reductions of above 15% with respect to nonflexible electric boiler based systems. At larger scales, higher T_{sink} up to 310 °C are also preferred since the lower specific CAPEX of the HTHP can be more favorably compensated by the increased performance and reduced electricity consumption from the system.

Innovative turbomachinery-based HTHP evolving CO_2 are currently under development and less commercial than the investigated Stirling based unit. However, when benchmarking the obtained attainable LCoH for similar system integration as shown in Ref. [13], similar techno-economic performance can be obtained.

Sensitivity Analyses. To assess the influence of some key assumptions, a set of sensitivity analyses has been performed. Figures 11 and 12 summarize the impact of the electricity price. Figure 11 shows the impact of the electricity price for an industry with a demand equivalent to profile B and a Q_{load} of 5 MW. The data for electricity price of 75 €/MWh, base case, are shown in Fig. 10 (mid chart). At lower electricity prices, the influence of the OPEX over the final LCoH is reduced. Therefore, the increase in CAPEX due to the HTHP and TES units is not paid back by the improved performance and reduced electrical consumption. Under the specific assumption at an average electricity price of 50 €/MWh, the investigated system attains similar performance as electric industrial steam generators. Thus, industrial site facing cheap and stable electricity prices would not largely benefit from the proposed solutions. In these cases, the increase in initial CAPEX and the system complexity would not be compensated by the improved performance, and a shift of the NG boiler toward simple electric boilers is suggested. Contrarily, at higher charging cost, a reduction of the OPEX is more beneficial and can compensate for the increase in the system CAPEX. Thus, the proposed system is cost-competitive also at lower available source side temperatures and can attain LCoH savings of about 15% with respect to electric boiler based BAU. Additionally, at higher electricity prices, the more cost-effective solutions are attained with the HTHP covering a larger share of thermal power and a higher level of MS preheating.

Figure 12 summarizes the influence of the specific thermal load on the attainable LCoH savings and required operating conditions for the HTHP for the different considered electricity prices. For thermal load lower than 15 MW and for electricity prices below 50 €/MWh, the addition of the HTHP is suggested only for a limited preheating of the MS with sink temperatures of about 200 °C. For thermal load higher than 15 MW and for electricity prices below 50 €/MWh, the

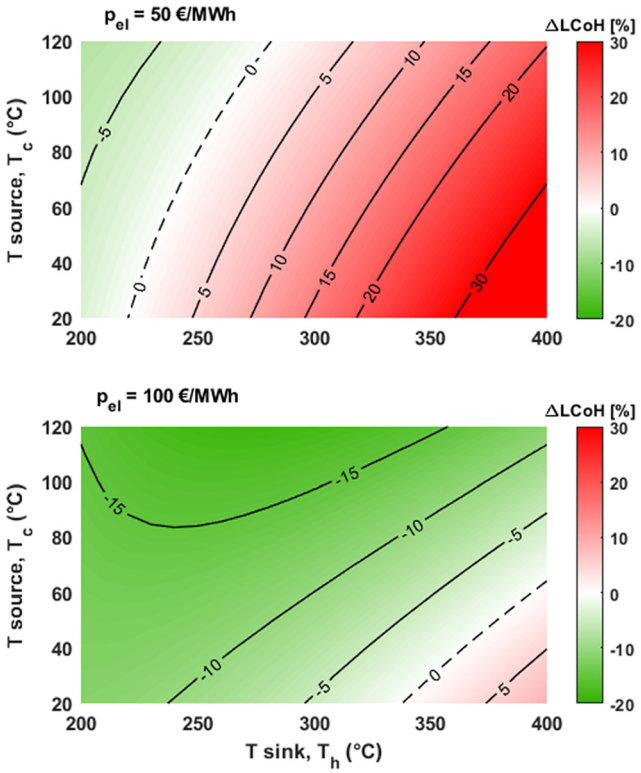

Fig. 11 Attainable LCoH savings for the proposed system for a Q_{load} of 5 MW and profile B and electricity price of 50 €/MWh and 100 €/MWh with respect to nonflexible electric boiler. The data for electricity price of 75 €/MWh are shown in Fig. 10.

HTHP addition can provide LCoH savings in the range 7–11%. However, its thermal power share, σ_{HTHP}, is limited to below 50%, as shown by a T_{sink} below 300 °C. For higher electricity prices (i.e., 75–100 €/MWh), larger LCoH savings can be attained, and the proposed system is largely cost-competitive even at small scales (below 1 MW). As highlighted for the base case, for higher thermal demand, the investigated system benefits from the reduced specific CAPEX of the HTHP and can attain lower LCoH at higher charging shares and T_{sink} from the HTHP. For average electricity prices of 100 €/MWh, maximum T_{sink} of about 330 °C are demanded. It should be also noted that, particularly at higher electricity prices, higher T_{sink} are required for thermal demand of about 10 MW. For thermal demand between 15 and 20 MW, a progressive slight reduction of the maximum T_{sink} is visible. This is caused by the fact that the increase of CAPEX of the HTHP at elevated T_{sink} is not compensated by the improved system performance, which is negatively affected by the reduction of COP. As in the base case, the maximum source side temperature, T_c, is always preferred.

Figure 13 shows the impact of the HTHP CAPEX on the system's maximum LCoH savings and required working temperatures for the HTHP, considering profile B and different thermal load. Specific LCoH maps for different source and sink temperatures of the HTHP for an industry with a Q_{load} of 5 MW are also reported in the Appendix. A HTHP CAPEX reduction of 25% leads to additional LCoH savings of about 2% for small industrial thermal load (<1 MW) and up to almost 4% for larger scale systems. A HTHP CAPEX equivalent to 75% of the values shown in Fig. 5 attain almost the same LCoH savings as for and electricity cost of 100 €/MW. Even in case of a HTHP equivalent to 125% of the base case, the proposed system is cost-competitive and can attain LCoH savings higher than 10%. At increased HTHP CAPEX, lower sink temperatures and thus lower share of MS preheating provided by the HTHP are preferred to limit the increase in CAPEX. It can also be highlighted that particularly for reduced CAPEX a plateau of the attainable LCoH reduction is reached for a thermal load between 15 and 20 MW. Similarly, as in the base scenario, maximum waste heat temperatures are preferred regardless of the HTHP specific CAPEX.

Figure 14 shows the impact of the real to Carnot efficiency ratio of the HTHP on the system's maximum LCoH savings and required working temperatures for the HTHP, considering profile B and different thermal load. Specific LCoH maps for different source and sink temperatures of the HTHP for an industry with a Q_{load} of 5 MW are also reported in the Appendix. Increased efficiency ratios lead to lower power consumptions and lower OPEX, which reflects in reduced LCoH. At higher thermal load, the effect of increased Carnot efficiency is more noticeable with LCoH savings that could be as high as 25% for thermal load higher than 20 MW. Similarly, at higher efficiency ratios, higher T_{sink} are suggested with peaks of around 350 °C for a thermal load between 10 and 15 MW. At lower efficiency ratios, the technical performance improvement provided by the HTHP is reduced. Therefore, its contribution is lowered with T_{sink} below 270 °C. These results support both initial assumptions that the proposed system is particularly suited for medium size industrial users and that serial integration of HTHP and EH can benefit the overall system performance limiting the HTHP to MS preheating.

Figure 15 shows the impact of available cheap charging hours on the system's maximum LCoH savings and required working temperatures for the HTHP, considering profile B and different

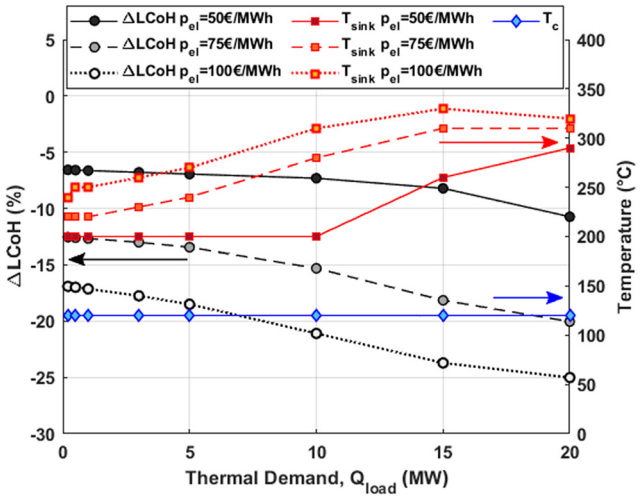

Fig. 12 Maximum attainable LCoH savings and required source and sink temperatures for the HTHP for three different constant electricity prices at profile B

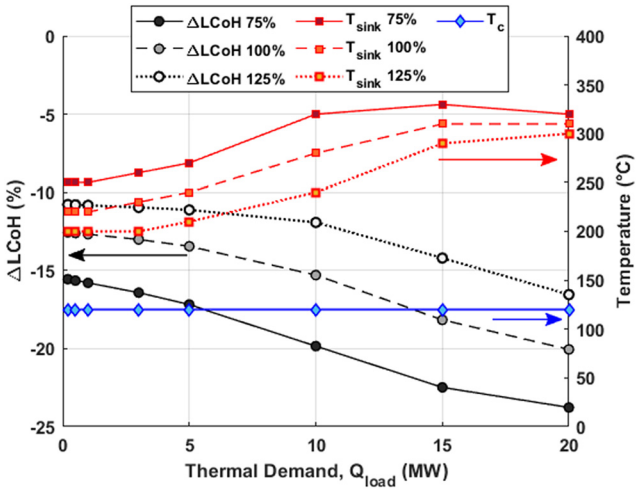

Fig. 13 Maximum attainable LCoH savings and required source and sink temperatures for the HTHP for different HTHP CAPEX at profile B

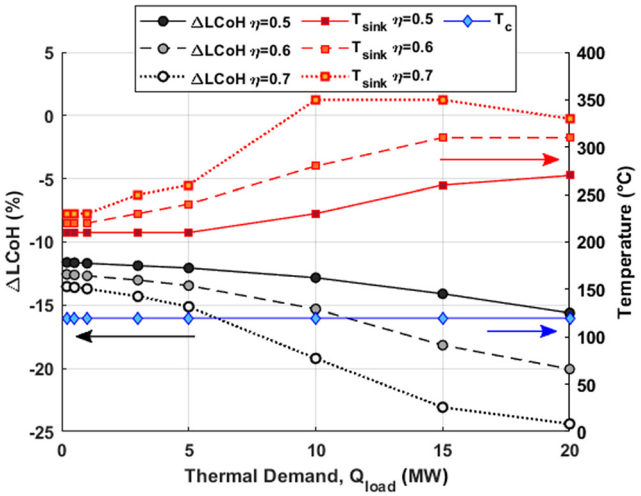

Fig. 14 Maximum attainable LCoH savings and required source and sink temperatures for the HTHP for different real to Carnot efficiency ratio of the HTHP at profile B

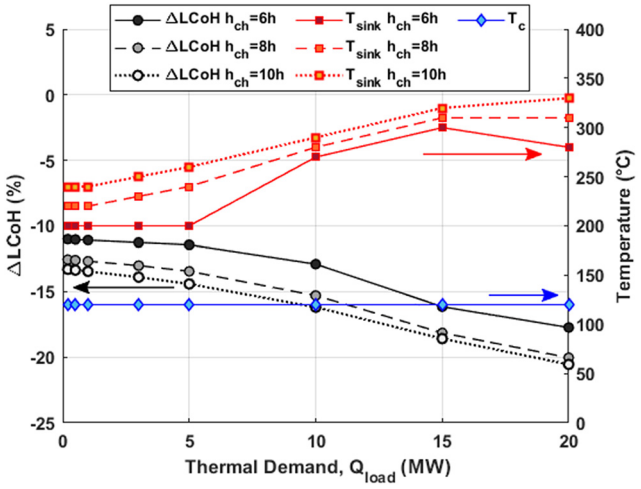

Fig. 15 Maximum attainable LCoH savings and required source and sink temperatures for the HTHP for different real to cheap charging hours at profile B

thermal load. Specific LCoH maps for different source and sink temperatures of the HTHP for an industry with a Q_{load} of 5 MW are also reported in the Appendix. Among the considered variables in the previous sensitivities, the amount of cheap charging hours has a lower influence on the performance of the proposed system. For h_{ch} equal to 10 h, an average additional LCoH savings of about 1% with respect to the base case can be seen. For longer h_{ch}, the required installed capacity for both the HTHP and EH is reduced limiting the CAPEX of the system. However, when long time period at cheap electricity are available, a simple electric boiler based solution without flexibility assets is also less expensive. At longer h_{ch}, higher T_{sink} are attainable by the HTHP since the additional CAPEX due to the increased working temperatures is compensated by the lower installed capacity. These results also suggest that the specific electricity pricing schemes should be carefully considered. Also, the proposed solution could become even more cost-effective in future scenarios with higher penetration of renewable energy causing cheaper electricity but higher cost fluctuations.

Conclusions

This work presents a comparative techno-economic performance assessment of a high-temperature heat pump integration within a molten salts based power-to-heat system for industrial heat flexible generation. Initially, a relevant high-temperature heat pump architecture and its integration within the power-to-heat system are presented, and the main results are reported in terms of required working conditions and temperature for the heat pump and thermal demand size. The impact of different industrial load profiles, electricity prices, heat pump capital cost, and heat pump real to Carnot efficiency ratio are also presented. From the results, the following main conclusions can be drawn:

- The proposed high-temperature heat pump integration in a molten salts based power-to-heat unit for industrial heat generation can provide up to more than 30% reduction in the overall electricity consumption with respect to electric boilers.
- The proposed system represents a cost-competitive solution against nonflexible electric boilers and levelized cost of heat savings higher than 15% can be attained particularly for industries with continuous thermal demand.
- Higher savings can be attained in case of higher electricity prices (around 75–100 €/MWh), even in small scale installations (with a thermal load lower than 1 MW).
- Capital investment reductions or improvements of the thermodynamic performance of the heat pump can lead to larger levelized cost of heat savings of about 15–20% against nonflexible electric boilers based systems.
- Maximum sink side temperatures for the high-temperature heat pump between 300 and 350 °C, thus limiting the role of the HTHP to MS preheating and requiring a EH to further boost the MS temperature, are required to maximize the system performance.

Future works will further expand this comparative assessment including more detailed modeling of the different components and their costs estimations. Such works will also consider different MS storage target temperatures and optimized dispatch strategies to fully investigated the influence of the specific electric price. Finally, future works will also address a full comparison with turbomachinery-based HTHP unit considering scalability of the machines.

Funding Data

- European Union's Horizon Europe research and innovation programme (Grant Agreement Nos. 101103552 and 101147078).
- Kyoto Group AS through the research project "Renewable Industrial Heat On-Demand" (RIHOND).

Data Availability Statement

The datasets generated and supporting the findings of this article are obtainable from the corresponding author upon reasonable request.

Nomenclature

BAU = business as usual
C = cost
CAPEX = capital expenditure
COP = coefficient of performance
EH = electric heater
h_{ch} = charging hours
h_{op} = operational hours
HTHP = high-temperature heat pump
LCoH = levelized cost of heat
MS = molten salt
NG = natural gas
OPEX = operational expenditure
p_{el} = electricity price
Q = thermal power
T_c = source side temperature

T_{sink} = sink side temperature
TES = thermal energy storage
W = electric power
Δ = reduction
η = net to Carnot COP ratio
σ = charging contribution share

Appendix

Figure S1 available in the Supplemental Materials on the ASME Digital Collection shows the impact of the HTHP CAPEX for an industry with a demand equivalent to profile B and a Q_{load} of 5 MW considering different source and sink side temperatures for the HTHP. The data for the base case can be seen in Fig. 10 (mid chart).

Figure S2 available in the Supplemental Materials shows the impact of the HTHP real to Carnot efficiency ratio for an industry with a demand equivalent to profile B and a Q_{load} of 5 MW considering different source and sink side temperatures for the HTHP. The data for the base case can be seen in Fig. 10 (mid chart).

Figure S3 available in the Supplemental Materials shows the impact of the available cheap charging hours for an industry with a demand equivalent to profile B and a Q_{load} of 5 MW considering different source and sink side temperatures for the HTHP. The data for the base case can be seen in Fig. 10 (mid chart).

References

[1] Ritchie, H., Roser, M., and Rosado, P., 2020, "CO_2 and Greenhouse Gas Emissions," OurWorldInData.org, accessed Jan. 3, 2024, https://ourworldindata.org/co2-and-other-greenhouse-gas-emissions

[2] United Nations, 2015, "Paris Agreement to the United Nations Framework Convention on Climate Change," United Nations, San Francisco, CA, T.I.A.S. No. 16-1104.

[3] IRENA, 2019, "Global Energy Transformation: A Roadmap to 2050," IRENA, Abu Dhabi.

[4] IRENA, 2019, "Renewable Power-to-Heat, Innovation Landscape Brief," IRENA, Abu Dhabi.

[5] Madeddu, S., Ueckerdt, F., Pehl, M., Peterseim, J., Lord, M., Kumar, K. A., Kruger, C., and Luderer, G., 2020, "The CO_2 Reduction Potential for the European Industry Via Direct Electrification of Heat Supply (Power-to-Heat)," Environ. Res. Lett., **15**(12), p. 124004.

[6] Schüwer, D., and Schneider, C., 2014, "Electrification of Industrial Process Heat: Long-Term Applications, Potentials and Impacts," ECEEE Ind. Summer Study Proc., 4-051-18, pp. 411–422.

[7] Arpagaus, C., Bless, F., Uhlmann, M., Schiffmann, J., and Bertsch, S. S., 2018, "High Temperature Heat Pumps: Market Overview, State of the Art, Research Status, Refrigerants, and Application Potentials," Energy, **152**, pp. 985–1010.

[8] Jiang, J., Hu, B., Wang, R. Z., Deng, N., Cao, F., and Wang, C., 2022, "A Review and Perspective on Industry High-Temperature Heat Pumps," Renewable Sustainable Energy Rev., **161**, p. 112106.

[9] Frate, G. F., Ferrari, L., and Desideri, U., 2020, "Multi-Criteria Investigation of a Pumped Thermal Electricity Storage (PTES) System With Thermal Integration and Sensible Heat Storage," Energy Convers. Manage., **208**, p. 112530.

[10] de Pee, A., Pinner, D., Roelofsen, O., Somers, K., Speelman, E., and Witteveen, M., 2018, "Decarbonization of Industrial Sectors: The Next Frontier," McKinsey & Company, New York.

[11] Trevisan, S., Buchbjerg, B., and Guedez, R., 2022, "Power-to-Heat for the Industrial Sector: Techno-Economic Assessment of a Molten Salt-Based Solution," Energy Convers. Manage., **272**, p. 116362.

[12] Yara International ASA, 2022, "Yara MOST," Yara International ASA, Oslo, Norway, accessed Jan. 3, 2024, https://www.yara.com/chemical-and-environmental-solutions/solar-power-molten-salt/

[13] Trevisan, S., Shamsi, S. S. M., Maccarini, S., Barberis, S., and Guedez, R., 2023, "Techno-Economic Assessment of CO_2-Based Power to Heat to Power Systems for Industrial Applications," ASME J. Eng. Gas Turbines Power, **145**(12), p. 121008.

[14] Høeg, A., Løver, K., and Vartdal, G., 2024, "Performance of a High-Temperature Industrial Heat Pump, Using Helium as Refrigerant," High Temperature Heat Pump Symposium, Copenhagen, Denmark, Jan. 23–24, pp. 2–7.

[15] Dany, H., 2023, "EHPA-Repower EU: Heat Pump and Paper Industry," accessed Jan. 3, 2024, https://www.ehpa.org/wp-content/uploads/2023/02/Atlas-CopCo_Cepi_EHPA_Presentation.pdf

[16] Wieringa, E., 2015, "Financial Feasibility of Using an Electric Steam Boiler in a Multifuel Steam Production Set and Providing Grid Flexibility," Master thesis, Construction Management and Engineering, Eindhoven University of Technology, Eindhoven, The Netherlands, pp. 1–113.

[17] Tax Foundation, 2024, "Carbon Taxes in Europe 2023," Tax Foundation, Bruxelles, Belgium, accessed Jan. 3, 2024, https://taxfoundation.org/data/all/eu/carbon-taxes-in-europe-2023/

[18] Pag, F., Jesper, M., and Jordan, U., 2021, "Reference Applications for Renewable Heat," Report No. D.A1.

[19] Guccione, S., Trevisan, S., Guedez, R., Laumert, B., Maccarini, S., and Traverso, A., 2022, "Techno-Economic Optimization of a Hybrid PV-CSP Plant With Molten Salt Thermal Energy Storage and Supercritical CO_2 Brayton Power Cycle," ASME Paper No. GT2022-80376.

[20] Kulhánek, M., and Dostál, V., 2011, "Thermodynamic Analysis and Comparison of Supercritical Carbon Dioxide Cycles," Supercritical CO_2 Power Cycle Symposium, San Antonio, TX, Feb. 26–29.

[21] Meng, F., Wang, E., Zhang, B., Zhang, F., and Zhao, C., 2019, "Thermo-Economic Analysis of Transcritical CO_2 Power Cycle and Comparison With Kalina Cycle and ORC for a Low-Temperature Heat Source," Energy Convers. Manage., **195**, pp. 1295–1308.

[22] Mctigue, J. D., Farres-Antunez, P., Neises, T., and White, A., 2020, "Supercritical CO_2 Heat Pumps and Power Cycles for Concentrating Solar Power," 26th SolarPACES Conference 2020, Golden, CO, Sept. 28–Oct. 2.

[23] Ho, C. K., Carlson, M., Garg, P., and Kumar, P., 2015, "Cost and Performance Tradeoffs of Alternative Solar-Driven s-CO_2 Brayton Cycle Configurations," ASME Paper No. ES2015-49467.

[24] Weiland, N. T., Lance, B. W., and Pidaparti, S. R., 2019, "sCO_2 Power Cycle Component Cost Correlations From DOE Data," ASME Paper No. GT2019-90493.